2007

Energy dispersion relations of spin-split subbands in a quantum wire and electrostatic modulation of carrier spin polarization

Sandipan Pramanik
Virginia Commonwealth University

Supriyo Bandyopadhyay
Virginia Commonwealth University

M. Cahay
University of Cincinnati - Main Campus

Energy dispersion relations of spin-split subbands in a quantum wire and electrostatic modulation of carrier spin polarization

Sandipan Pramanik and Supriyo Bandyopadhyay*
Department of Electrical and Computer Engineering, Virginia Commonwealth University, Richmond, Virginia 23284, USA

Marc Cahay
Department of Electrical and Computer Engineering, University of Cincinnati, Cincinnati, Ohio 45221, USA
(Received 16 May 2007; revised manuscript received 23 July 2007; published 26 October 2007)

We numerically calculate the energy dispersion relations of the spin-split subbands in a quantum wire subjected to a transverse magnetic field in the presence of Rashba and Dresselhaus spin-orbit interactions. The spin splitting energy at zero wave vector is found to be neither equal to the bare Zeeman splitting nor linear in the magnetic field in any subband. This happens because the expectation value of the spin angular momentum operator varies along the width of the wire, causing a spatial modulation of the spin density. We also show that spin splitting energy is subband dependent and has a complex dependence on the external magnetic field. In some subbands, it can vanish entirely at nonzero values of the external magnetic field. The effective spin polarization of carriers in any subband can be changed in both magnitude and sign with an external electrostatic potential, applied, for example, via a gate terminal. This has practical applications in quantum computing and other areas.

DOI: 10.1103/PhysRevB.76.155325 PACS number(s): 72.25.Rb, 72.25.Mk, 72.25.Hg, 72.25.Dc

I. INTRODUCTION

The subband structure of quasi-one-dimensional systems, with strong spin-orbit interaction, has been extensively studied in the past.[1–12] It is well known that in the absence of an external magnetic field, the Rashba and Dresselhaus spin-orbit interactions lift the spin degeneracy in any subband at nonzero wave vectors ($k \neq 0$). Additionally, if an external magnetic field (B) is present, then the spin degeneracy is lifted at all wave vectors, including $k=0$, because of the wave-vector-independent Zeeman splitting $\Delta = g\mu_B B$, where g is the Landé g factor in the material and μ_B ($=e\hbar/2m_0$) is the Bohr magneton. As a result, it is natural to expect that in the presence of B, the zero-k spin splitting in any subband will be given by the Zeeman term alone[13] since the spin-orbit interactions vanish at $k=0$. Analytical models based on zeroth order perturbation treatment,[4–6] support this picture.

In this work, we report an exact numerical solution of the nonrelativistic Pauli equation in a quantum wire subjected to a transverse magnetic field in the presence of Rashba and Dresselhaus spin-orbit interactions. We show that in the presence of a spin-orbit interaction, the zero-k spin splitting energy in any subband (i) is not equal to the Zeeman splitting $g\mu_B B$ and (ii) is not even linear in B. Moreover, the zero-k splitting depends on the spin-orbit interaction strength which can be varied with an electrostatic potential.[14,15] As a result, the zero-k spin splitting in any subband can be modulated by an external gate potential, allowing us to alter the spin polarization of carriers in the quantum wire by electrostatic means.

II. THEORY

Let us consider a semiconductor quantum wire with a rectangular cross section, as shown in Fig. 1. The axis of the wire is along $\hat{x}$, while a symmetry-breaking electric field $E_y\hat{y}$ and an external magnetic field $B\hat{y}$ ($B>0$) act along $\hat{y}$. Since the electric field breaks the spatial inversion symmetry along $\hat{y}$, it induces a Rashba spin-orbit interaction[16] in the quantum wire. The strength of this interaction can be varied with an electrostatic potential applied to a top gate terminal, which changes the electric field $E_y\hat{y}$. Additionally, if the wire material is an inversion-asymmetric zinc-blende compound (e.g., III-V semiconductors such as GaAs), then there is a bulk inversion asymmetry present in the microscopic crystal potential, which induces the Dresselhaus spin-orbit interaction.[17] The strength of the latter interaction depends on the transverse dimensions of the quantum wire, which can be varied with a side gate (or split gate) potential.[15] Thus, the strengths of both the Rashba and the Dresselhaus spin-orbit interactions in the quantum wire can be varied with external gate potentials. We will show that this will vary the zero-k spin splitting energy in any subband.

For the sake of simplicity, assume that the quantum wire axis is along the [100] crystallographic direction. In that

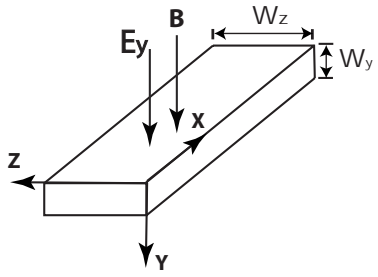

FIG. 1. Geometry of the quantum wire. For our numerical calculations, we assumed that the width of the wire along the z direction is 100 nm and the thickness of the wire along the y direction is much smaller so that only the lowest transverse subband in the y direction is occupied. The y-directed electric field E_y induces a Rashba spin-orbit interaction in the channel, and B is an external magnetic field, also applied in the y direction.

case, the single particle effective mass Hamiltonian describing an electron in the quantum wire is given by

$$H = \frac{(\vec{p} + e\vec{A})^2}{2m^*} + V(y) + V(z) - \frac{g\mu_B \vec{B} \cdot \vec{\sigma}}{2} + H_R + H_D, \quad (1)$$

where H_R is the Rashba interaction Hamiltonian, H_D is the Dresselhaus interaction Hamiltonian, m^* is the effective mass of an electron, and $\vec{A}$ is the vector potential associated with the external magnetic field $B\hat{y}$. The quantities $V(y)$ and $V(z)$ are the electrostatic confinement potentials along the y and z directions, respectively. We apply hard wall boundary conditions,

$$V(y) = -eE_y y \quad \text{for } 0 \leqslant y \leqslant W_y$$

$$= \infty \text{ otherwise}, \quad (2a)$$

$$V(z) = 0 \quad \text{for } 0 \leqslant z \leqslant W_z$$

$$= \infty \text{ otherwise}, \quad (2b)$$

where W_y and W_z are the dimensions of the quantum wire in the $\hat{y}$ and $\hat{z}$ directions, respectively.

Using the Landau gauge $\vec{A} = (Bz, 0, 0)$, the Rashba Hamiltonian H_R can be written in the following form:

$$H_R = \frac{\eta_R}{\hbar} \hat{y} \cdot [\vec{\sigma} \times (\vec{p} + e\vec{A})] = \frac{\eta_R}{\hbar} [\sigma_z (p_x + eBz) - \sigma_x p_z], \quad (3)$$

where η_R is the Rashba spin-orbit coupling constant that can be varied with the gate electric field E_y. Note that the potential discontinuities at the boundaries ($y=0, W_y$ and $z=0, W_z$) result in additional electric fields. However, as shown in Ref. 18, these electric fields at the edges of the quantum wire do not contribute to spin-orbit coupling. If the quantum wire is contacted by two metallic electrodes (as in transport experiments), an additional spin-orbit effect can originate in the vicinity of the metal/semiconductor junctions due to Schottky electric fields. Since we are not studying transport, we ignore the presence of any metallic contacts, and hence this effect is not relevant in the present case. As a result, we can assume that the quantity η_R depends only on E_y and is independent of the spatial coordinate x, y, or z. Space charge effects can still introduce some spatial variation in η_R. In this study, we ignore this effect since its inclusion adds considerably to the computational burden. In any case, it would have only made a quantitative (but no qualitative) difference to the result.

The Dresselhaus Hamiltonian is given by

$$H_D = \frac{\eta_D}{\hbar} \vec{\sigma} \cdot \vec{\kappa}, \quad (4)$$

where η_D is the Dresselhaus spin-orbit coupling constant (which depends on W_y and W_z and, therefore, can be varied with a split gate potential that controls W_z) and $\vec{\kappa} = (\kappa_x, \kappa_y, \kappa_z)$. If we assume that W_y is so small that $\langle p_y^2 \rangle \gg \langle p_x^2 \rangle, \langle p_z^2 \rangle$, then we can write the components of $\vec{\kappa}$ in a simplified form,

$$\kappa_x = \frac{1}{2}[(p_x + eA_x)\{(p_y + eA_y)^2 - (p_z + eA_z)^2\} + \{(p_y + eA_y)^2 - (p_z + eA_z)^2\}(p_x + eA_x)]$$

$$= \frac{1}{2}[(p_x + eBz)(p_y^2 - p_z^2) + (p_y^2 - p_z^2)(p_x + eBz)]$$

$$\approx (p_x + eBz)p_y^2, \quad (5a)$$

$$\kappa_y = \frac{1}{2}[(p_y + eA_y)\{(p_z + eA_z)^2 - (p_x + eA_x)^2\} + \{(p_z + eA_z)^2 - (p_x + eA_x)^2\}(p_y + eA_y)]$$

$$= p_y\{p_z^2 - (p_x + eBz)^2\}, \quad (5b)$$

$$\kappa_z = \frac{1}{2}[(p_z + eA_z)\{(p_x + eA_x)^2 - (p_y + eA_y)^2\} + \{(p_x + eA_x)^2 - (p_y + eA_y)^2\}(p_z + eA_z)]$$

$$\approx -p_z p_y^2. \quad (5c)$$

Thus, the Dresselhaus Hamiltonian can be approximated as

$$H_D \approx (\eta_D/\hbar) p_y^2 [\sigma_x (p_x + eBz) - \sigma_z p_z]. \quad (6)$$

Here, we have neglected the $\sigma_y \kappa_y$ term since $\langle p_y \rangle = 0$.

The total Hamiltonian can be written as

$$H = H_0 I - \frac{g}{2}\mu_B B\sigma_y + \frac{\eta_R}{\hbar}[\sigma_z (p_x + eBz) - \sigma_x p_z] + (\eta_D/\hbar) p_y^2 [\sigma_x (p_x + eBz) - \sigma_z p_z], \quad (7)$$

where I is 2×2 identity matrix and

$$H_0 = \frac{p_x^2 + p_y^2 + p_z^2}{2m^*} + \frac{e^2 B^2 z^2}{2m^*} + \frac{eBzp_x}{m^*} + V(y) + V(z). \quad (8)$$

We intend to calculate the energy eigenvalues (E) and eigenfunctions (Ψ) of the Pauli equation $H\Psi = E\Psi$, where H is given by Eq. (7). Since the entire Hamiltonian H is translationally invariant along the x coordinate, we can write $\Psi(x,y,z) = \exp[iq_x x]\phi(y)\zeta(z)$. Note that the total wave function $\Psi(x,y,z)$ must be a two-component spinor: $\Psi(x,y,z) = [\Psi_\alpha(x,y,z), \Psi_\beta(x,y,z)]^T$, where the superscript T stands for transpose.

Since the coefficients of the Pauli matrices in the Hamiltonian H [Eq. (7)] do not involve the x and y coordinates, we can write $\Psi(x,y,z) = [\Psi_\alpha(x,y,z), \Psi_\beta(x,y,z)]^T \equiv \exp[iq_x x]\phi(y)[\zeta_\alpha(z), \zeta_\beta(z)]^T$, where $\zeta(z) = [\zeta_\alpha(z), \zeta_\beta(z)]^T$. Normalization condition requires $\int_{-\infty}^{\infty}(|\zeta_\alpha(z)|^2 + |\zeta_\beta(z)|^2)dz = 1$.

Spatially averaging both sides of the Pauli equation over x and y coordinates, we get

$$E\zeta(z) = \left[\tilde{H}_0 I - \frac{g}{2}\mu_B B\sigma_y + \eta_R\left\{\left(q_x + \frac{eBz}{\hbar}\right)\sigma_z + i\sigma_x\frac{d}{dz}\right\} + \gamma_D\left\{\left(q_x + \frac{eBz}{\hbar}\right)\sigma_x + i\sigma_z\frac{d}{dz}\right\}\right]\zeta(z)$$
$$= \{\tilde{H}_0 I + H_S\}\zeta(z), \tag{9}$$

where

$$\gamma_D = \eta_D\langle p_y^2\rangle_n,$$

$$\tilde{H}_0 = \frac{\hbar^2 q_x^2}{2m^*} - \frac{\hbar^2}{2m^*}\frac{d^2}{dz^2} + \frac{eBz\hbar q_x}{m^*} + \frac{e^2B^2z^2}{2m^*} + \epsilon_n + V(z),$$

$$H_S = -(g/2)\mu_B B\sigma_y + \eta_R\left[\left(q_x + \frac{eBz}{\hbar}\right)\sigma_z + i\sigma_x\frac{d}{dz}\right] + \gamma_D\left[\left(q_x + \frac{eBz}{\hbar}\right)\sigma_x + i\sigma_z\frac{d}{dz}\right],$$

$$\langle p_y^2\rangle_n = \int_{-\infty}^{\infty}\phi_n^*(y)[-\hbar^2\partial^2/\partial y^2]\phi_n(y)dy, \tag{10}$$

and

$$\left[-\frac{\hbar^2}{2m^*}\frac{d^2}{dy^2} + V(y)\right]\phi_n(y) = \epsilon_n\phi_n(y), \tag{11}$$

where $V(y)$ is given by Eq. (2a) and n is the index of the transverse subband in the y direction.

Equation (9) can be written compactly as

$$\{\mathbf{B}q_x + \mathbf{C}\}\zeta(z) = \mathbf{A}q_x^2\zeta(z), \tag{12}$$

where the 2×2 matrices $\mathbf{A}$, $\mathbf{B}$, and $\mathbf{C}$ are given by

$$\mathbf{A} = -\frac{\hbar^2}{2m^*}I, \tag{13}$$

$$\mathbf{B} = eBz\frac{\hbar}{m^*}I + \eta_R\sigma_z + \gamma_D\sigma_x, \tag{14}$$

and

$$\mathbf{C} = \left[-\frac{\hbar^2}{2m^*}\frac{\partial^2}{\partial z^2} + \epsilon_n + V(z) + \frac{e^2B^2z^2}{2m^*} - E\right]I - \frac{g}{2}\mu_B B\sigma_y + \frac{eBz}{\hbar}[\eta_R\sigma_z + \gamma_D\sigma_x] + i\frac{d}{dz}[\eta_R\sigma_x + \gamma_D\sigma_z]. \tag{15}$$

In order to find the energy dispersion relations of the spin-split subbands in the quantum wire, we have to find the values of the wave vector q_x that satisfy Eq. (12) for a given value of energy E. We then repeat this procedure for various values of E to find the dispersion relation (E versus q_x). Unfortunately, this is not straightforward since Eq. (12) is not an eigenequation in q_x because it is nonlinear in q_x. We therefore have to convert Eq. (12) to an eigenequation in q_x using the following procedure.

Let

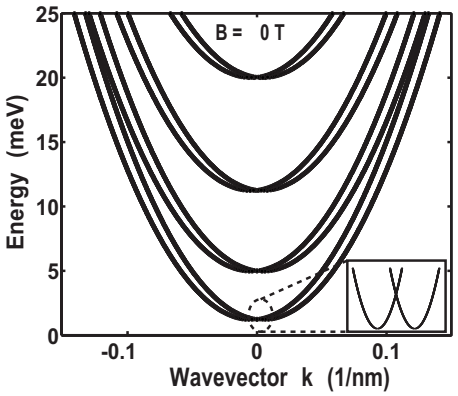

FIG. 2. Energy dispersion relation (E-k plot) in a quantum wire of width 100 nm for $B=0$ T. The material is assumed to be InAs with electron effective mass 0.03 times the free electron mass and the Landé g factor=−15. The Rashba and Dresselhaus interaction strengths are $\eta_R=2\gamma_D=10^{-11}$ eV m.

$$\lambda(z) = q_x\zeta(z) = q_x\begin{bmatrix}\zeta_\alpha(z)\\ \zeta_\beta(z)\end{bmatrix}. \tag{16}$$

Using Eq. (16), we can rewrite Eq. (12) as an eigenequation in q_x,

$$\begin{bmatrix}\mathbf{0} & \mathbf{I}\\ \{\mathbf{A}^{-1}\mathbf{C}\} & \{\mathbf{A}^{-1}\mathbf{B}\}\end{bmatrix}\begin{bmatrix}\zeta(z)\\ \lambda(z)\end{bmatrix} = q_x\begin{bmatrix}\zeta(z)\\ \lambda(z)\end{bmatrix}. \tag{17}$$

Equation (17) can be solved numerically (for any energy E) subject to the boundary condition

$$\zeta(z=0) = \zeta(z=W_z) = 0$$

to find the corresponding values of q_x in different subbands. This procedure, adapted from Ref. 19, yields the dispersion relation E versus q_x in different subbands.

Using the above procedure, we have found q_x^m, $\zeta_{\alpha,m}(z)$, and $\zeta_{\beta,m}(z)$ for any arbitrary value of E in different subbands m. The dispersion relations obtained from these solutions, for various values of external magnetic field B and for fixed Rashba and Dresselhaus interaction strengths $\eta_R=2\gamma_D$

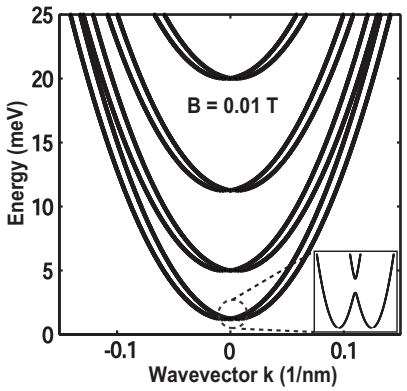

FIG. 3. E-k plot for $B=0.01$ T. The magnetic field is low enough that the lower spin-split subband has a camelback shape. All other parameters are the same as in Fig. 2.

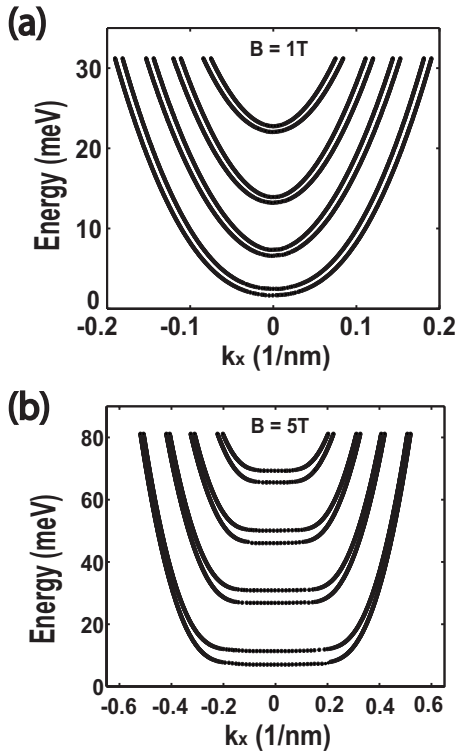

FIG. 4. E-k plot for (a) $B=1$ T and (b) $B=5$ T. All other parameters are the same as in Fig. 2. The camelback shape has disappeared for these high magnetic fields, and at 5 T, the subband bottoms are flat, indicating the formation of closed Landau orbits in the quantum wire.

$=10^{-11}$ eV m, are shown in Figs. 2–4 for a quantum wire of width 100 nm. We plotted the dispersion relations as energy E versus the shifted wave vector $k_x \rightarrow q_x + eBW_z/(2\hbar)$, so that the dispersion relations are always centered around $k_x=0$ for arbitrary magnetic field strengths. We assumed that the quantum wire material is InAs with electron effective mass $=0.03$ times the free electron mass and the Landé g factor equal to -15.

III. RESULTS AND DISCUSSION

From Figs. 2–4, we note that the dispersion relations are strongly dependent on the externally applied magnetic field B. For $B=0$ (Fig. 2), we obtain two horizontally displaced parabolas with spin degeneracy only at $k=k_x=0$. For small nonzero values of B (Fig. 3), the spin degeneracy is lifted for all k and the lower spin band develops a "camelback" shape as long as B is less than a critical value.[4–6,20] For larger values of B, the camelback shape disappears, as shown in Figs. 4(a) and 4(b). Note that at very high values of B, the dispersion curves have nearly flat bottoms which correspond to states with virtually no translational velocity ($\langle v_x \rangle \approx 0$). These correspond to the closed Landau orbits.

In Figs. 5(a) and 5(b), we show the real and imaginary parts of the two-component wave function $[\zeta_\alpha(z), \zeta_\beta(z)]^T$ for an electron with arbitrarily chosen energy $E_0=15$ meV. The magnetic flux density $B=5$ T. In this case, only one spin-

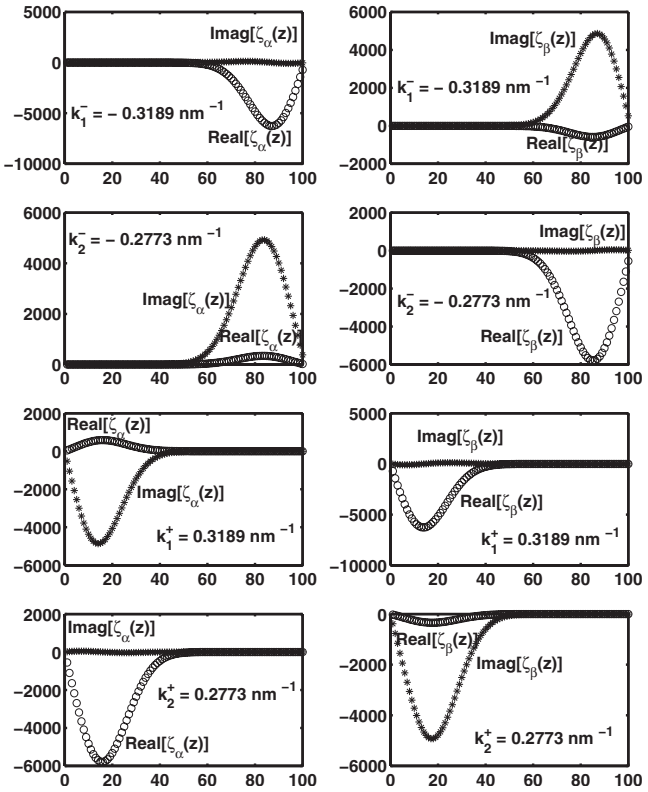

FIG. 5. Edge states in a quantum wire. The z dependence of the real (denoted by "o") and imaginary parts (denoted by " *") of the two components of the wave function $[\zeta_\alpha(z), \zeta_\beta(z)]^T$ are shown. The electron energy $E_0=15$ meV and magnetic flux density $B=5$ T. Only one spin-split subband in the quantum wire is below this energy. The wave vectors corresponding to this energy in the two spin-split levels are $k_1^{\pm}=\pm 0.3189$ nm^{-1} (lower level) and $k_2^{\pm}=\pm 0.2773$ nm^{-1} (upper level). The wave functions are skewed to the left or right edge of the quantum wire, depending on whether the electrons are forward or backward traveling, because of the Lorentz force that pushes electrons toward one or the other edge. The horizontal axes in all figures are in nanometers.

split subband lies below E_0 and the higher subbands are evanescent. The corresponding wave vectors in the two (nonevanescent) spin-split levels are given by $k_1^{\pm}=\pm 0.3189$ nm^{-1} (lower level) and $k_2^{\pm}=\pm 0.2773$ nm^{-1} (upper level). In Fig. 5, we plot the two components $\zeta_\alpha(z)$ and $\zeta_\beta(z)$ separately for the wave vector values $k_1^{\pm}$ and $k_2^{\pm}$. Note that the wave functions are skewed to the left or right depending on the direction of the electron velocity. This happens because the Lorentz force associated with the magnetic field pushes moving electrons toward either the left or the right edge of the quantum wire depending on whether the electron is traveling forward or backward along the length of the quantum wire. In other words, these wave functions represent the well known "edge states."

Figure 5 also indicates that in the presence of a spin-orbit interaction, the z component of the wave function, $[\zeta_{\alpha,m}(z), \zeta_{\beta,m}(z)]^T$, in any subband m *cannot* be written as the product of a space dependent part and an eigenspinor, i.e.,

$$\begin{bmatrix} \zeta_{\alpha,m}(z) \\ \zeta_{\beta,m}(z) \end{bmatrix} \neq \zeta_m(z) \begin{bmatrix} \alpha_m \\ \beta_m \end{bmatrix}, \tag{18}$$

where α_m and β_m are z independent. This implies that the expectation value of the spin angular momentum operator is *z-dependent*. The expectation value is defined as $(\hbar/2)\vec{S}$, where

$$\vec{S} = S_x\hat{x} + S_y\hat{y} + S_z\hat{z},$$

$$\vec{S}_i = [\zeta_\alpha^*(z), \zeta_\beta^*(z)][\sigma_i][\zeta_\alpha(z), \zeta_\beta(z)]^T,$$

$$S_i = \frac{\vec{S}_i}{\sqrt{\sum_i \vec{S}_i^2}}, \quad i = x, y, z. \tag{19}$$

This spatial variation of spin angular momentum is shown in Fig. 6. Here, we plot the expectation values of the spin components [Eq. (19)] as a function of the z coordinate for the four wave vector states $k_1^\pm$ and $k_2^\pm$ corresponding to $E_0 = 15$ meV and $B = 5$ T. From this figure, we observe that the expectation value of the spin angular momentum $(\hbar/2)\vec{S} = (\hbar/2)[S_x\hat{x} + S_y\hat{y} + S_z\hat{z}]$ indeed changes with the z coordinate, resulting in a spatial modulation of the spin density along the width of the wire. A similar phenomenon has also been discussed in Ref. 21.

According to Fig. 6, the spin of an electron, in the presence of a spin-orbit interaction and external transverse magnetic field B, is not only determined by its wave vector k but also by its spatial location along z. This happens because the spin-orbit Hamiltonian H_S in Eq. (10) is z dependent. Consequently, the pseudomagnetic field caused by spin-orbit interaction is also z dependent. The net magnetic field that an electron experiences is the vector sum of the pseudomagnetic field and the external magnetic field. This net field varies with the coordinate z. Since spins will align parallel or antiparallel to the net field, the spin orientation will vary with z. In the following discussion, we will argue that as a result of this spatial modulation effect, zero-k spin splitting (a) is no longer equal to Zeeman splitting $g\mu_B B$, (b) is not even linear in B, and (c) depends on the spin-orbit coupling constants η_R and γ_D, which determine the strength of the pseudomagnetic field.

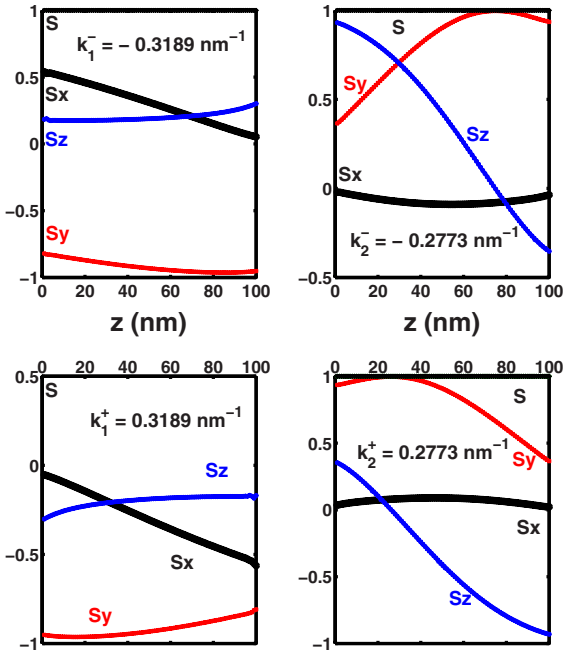

FIG. 6. (Color online) The expectation values of the spin components [see Eq. (19)] S_x, S_y, and S_z and $S = \sqrt{S_x^2 + S_y^2 + S_z^2}$ as functions of the z coordinate. We have plotted the spin components in the four nonevanescent bands when the electron energy $E_0 = 15$ meV and $B = 5$ T. For these values of E_0 and B, the corresponding wave vectors are $k_1^\pm = \pm 0.3189$ nm^{-1} and $k_2^\pm = \pm 0.2773$ nm^{-1}.

If the two-component electron wave function could have been expressed as the product of a spatially varying scalar and a spatially invariant spinor, then the inequality sign in Eq. (18) would have been replaced with an equality. In that case, the expectation value of the spin angular momentum would be z independent since the spinor is z independent. For that situation, it can be shown from Eq. (9) that if we neglect coupling between subbands (assuming that the energy separation between subbands is large enough), then the zero-k spin splitting energy in the mth subband will be

$$\Delta_{k=0}^m = 2\sqrt{\left(\frac{\eta_R^2 + \gamma_D^2}{\hbar^2}\right)\left[e^2B^2\left(\langle z^m\rangle - \frac{W_z}{2}\right)^2 + \langle p_z^m\rangle^2\right] - \frac{4\gamma_D\eta_R eB}{\hbar^2}\left(\langle z^m\rangle - \frac{W_z}{2}\right)\langle p_z^m\rangle + \left(\frac{g\mu_B B}{2}\right)^2}. \tag{20}$$

Here, $\langle z^m\rangle = \int_{-\infty}^{\infty} dz\,\zeta_m^*(z) z \zeta_m(z) = W_z/2$ (evaluated at $k_x = 0$) and $\langle p_z^m\rangle = \int_{-\infty}^{\infty} dz\,\zeta_m^*(z)[-i\hbar(\partial/\partial z)]\zeta_m(z) = 0$ (due to the confinement along the z direction). Therefore, if Eq. (18) were an equality instead of an inequality, then

$$\Delta_{k=0}^m = g\mu_B B, \tag{21}$$

which is the simple Zeeman splitting.

However, since inequality (18) is valid (see Fig. 5), which makes the expectation value of the spin angular momentum dependent on the z coordinate (see Fig. 6), Eq. (21) will not hold and the actual zero-k spin splitting must be calculated from Eq. (9).

It follows from Eq. (9) that if we neglect coupling between subbands, then the energy eigenvalues are given by

$$E_m = \langle \tilde{H}_0 \rangle_m + \langle H_S \rangle_m, \tag{22}$$

where m is a composite subband index that labels subbands formed due to confinement in both y and z directions, and

$$\langle \tilde{H}_0 \rangle_m = \int_{-\infty}^{\infty} [\zeta^*_{\alpha,m}(z), \zeta^*_{\beta,m}(z)] \tilde{H}_0 I [\zeta_{\alpha,m}(z), \zeta_{\beta,m}(z)]^T dz$$

$$= \int_{-\infty}^{\infty} [\zeta^*_{\alpha,m}(z) \tilde{H}_0 \zeta_{\alpha,m}(z) + \zeta^*_{\beta,m}(z) \tilde{H}_0 \zeta_{\beta,m}(z)] dz,$$

$$\langle H_S \rangle_m = -\frac{\gamma_D}{\hbar}[\langle p_{\alpha,m} \rangle - \langle p_{\beta,m} \rangle] + \frac{\eta_R e B}{\hbar}[\langle z_{\alpha,m} \rangle - \langle z_{\beta,m} \rangle]$$

$$- \frac{g\mu_B B}{2}\langle S_y \rangle + \eta_R k_x \langle S_z \rangle + \gamma_D k_x \langle S_x \rangle$$

$$- \frac{\eta_R}{\hbar}[\langle p_{\beta\alpha,m} \rangle + \langle p_{\alpha\beta,m} \rangle] + \frac{\gamma_D e B}{\hbar}[\langle z_{\beta\alpha,m} \rangle + \langle z_{\alpha\beta,m} \rangle]$$

$$\equiv -\frac{\gamma_D}{\hbar}[\langle p_{\alpha,m} \rangle - \langle p_{\beta,m} \rangle] + \frac{\eta_R e B}{\hbar}[\langle z_{\alpha,m} \rangle - \langle z_{\beta,m} \rangle]$$

$$- \frac{\eta_R}{\hbar}[\langle p_{\beta\alpha,m} \rangle + \langle p_{\alpha\beta,m} \rangle]$$

$$+ \frac{\gamma_D e B}{\hbar}[\langle z_{\beta\alpha,m} \rangle + \langle z_{\alpha\beta,m} \rangle] + \langle \vec{S} \rangle \cdot \vec{n}_s, \tag{23}$$

with

$$\langle p_{\alpha,m(\beta,m)} \rangle = \int_{-\infty}^{\infty} \left(\zeta^*_{\alpha,m(\beta,m)} (-i\hbar) \frac{d\zeta_{\alpha,m(\beta,m)}}{dz} \right) dz, \tag{24a}$$

$$\langle z_{\alpha,m(\beta,m)} \rangle = \int_{-\infty}^{\infty} (\zeta^*_{\alpha,m(\beta,m)} z \zeta_{\alpha,m(\beta,m)}) dz, \tag{24b}$$

$$\langle p_{\beta\alpha,m(\alpha\beta,m)} \rangle = \int_{-\infty}^{\infty} \left(\zeta^*_{\alpha,m(\beta,m)} (-i\hbar) \frac{d\zeta_{\beta,m(\alpha,m)}}{dz} \right) dz, \tag{24c}$$

$$\langle z_{\beta\alpha,m(\alpha\beta,m)} \rangle = \int_{-\infty}^{\infty} (\zeta^*_{\alpha,m(\beta,m)} z \zeta_{\beta,m(\alpha,m)}) dz, \tag{24d}$$

$$\langle S_i \rangle = \int_{-\infty}^{\infty} \zeta^\dagger(z) \sigma_i \zeta(z) dz \equiv \int_{-\infty}^{\infty} \vec{S}_i(z) dz, \quad i = x, y, z, \tag{24e}$$

$$\vec{n}_s = \gamma_D k_x \hat{x} - \frac{g\mu_B B}{2}\hat{y} + \eta_R k_x \hat{z}, \tag{24f}$$

$$\langle \vec{S} \rangle = \langle S_x \rangle \hat{x} + \langle S_y \rangle \hat{y} + \langle S_z \rangle \hat{z}. \tag{24g}$$

For $k_x = 0$, and in the limit of a weak spin-orbit interaction, we can write $\langle \vec{S} \rangle \cdot \vec{n}_s \approx \pm (g\mu_B B/2)$, where the "+" and "−" signs correspond to upper and lower spin-split levels, respectively.

Now, from Eq. (23), we find that if we neglect coupling between subbands, then, in the limit of a weak spin-orbit interaction, the zero-k spin splitting energy will be given by

$$\Delta^m_{k=0} = -\frac{\gamma_D}{\hbar}[\langle p_{\alpha,m} \rangle_U - \langle p_{\beta,m} \rangle_U] + \frac{\eta_R e B}{\hbar}[\langle z_{\alpha,m} \rangle_U - \langle z_{\beta,m} \rangle_U]$$

$$- \frac{\eta_R}{\hbar}[\langle p_{\beta\alpha,m} \rangle_U + \langle p_{\alpha\beta,m} \rangle_U]$$

$$+ \frac{\gamma_D e B}{\hbar}[\langle z_{\beta\alpha,m} \rangle_U + \langle z_{\alpha\beta,m} \rangle_U] + \frac{\gamma_D}{\hbar}[\langle p_{\alpha,m} \rangle_L - \langle p_{\beta,m} \rangle_L]$$

$$- \frac{\eta_R e B}{\hbar}[\langle z_{\alpha,m} \rangle_L - \langle z_{\beta,m} \rangle_L] + \frac{\eta_R}{\hbar}[\langle p_{\beta\alpha,m} \rangle_L + \langle p_{\alpha\beta,m} \rangle_L]$$

$$- \frac{\gamma_D e B}{\hbar}[\langle z_{\beta\alpha,m} \rangle_L + \langle z_{\alpha\beta,m} \rangle_L] + g\mu_B B, \tag{25}$$

where the subscripts U and L refer to the upper and lower spin-split states in any subband m. Clearly, the zero-k spin splitting energy $\Delta^m_{k=0} \neq g\mu_B B$ because of the first four terms in the above equation, which are nonvanishing. Moreover, since the $\langle p \rangle$-s and the $\langle z \rangle$-s depend on B, $\Delta^m_{k=0}$ is *not* linear in B. We emphasize that although we neglected coupling between subbands to arrive at the analytical form in the preceding equation, we did not neglect this coupling when we calculated the dispersion relations in Figs. 2–4. Those results, obtained by solving Eq. (17) numerically, are exact. The quantities η_R, γ_D, and B not only appear as coefficients in Eq. (25), but they also influence the quantities within the square brackets.

In Fig. 7(a), we plot the numerically computed zero-k spin splitting energy $\Delta'^{,m}_{k=0}$ (normalized to $g\mu_B B$) in the three lowest subbands ($m = 1, 2, 3$) as a function of B, for fixed values of η_R and γ_D. As discussed before, the zero-k spin splitting energy is clearly *not* the bare Zeeman splitting $g\mu_B B$ and is not even linear in B (except at very high values of B when the Zeeman term dominates). For subband 1, the spin splitting energy increases with increasing B. For subbands 2 and 3, the spin splitting energy decreases with increasing B, crosses zero, and then changes sign to become negative. To elucidate this strange behavior, we have plotted in Fig. 7(b) how the spin-split subband bottom energies evolve with increasing B. As $|B|$ increases, the energy at the bottom of each level increases because of the increasing magnetostatic confinement in the wire. The rate of this increase is, however, different for different subbands (because their wave functions are different) and also different for the two levels within each subband because of spin-orbit interaction. It so happens that for the chosen parameters (the wire dimension,

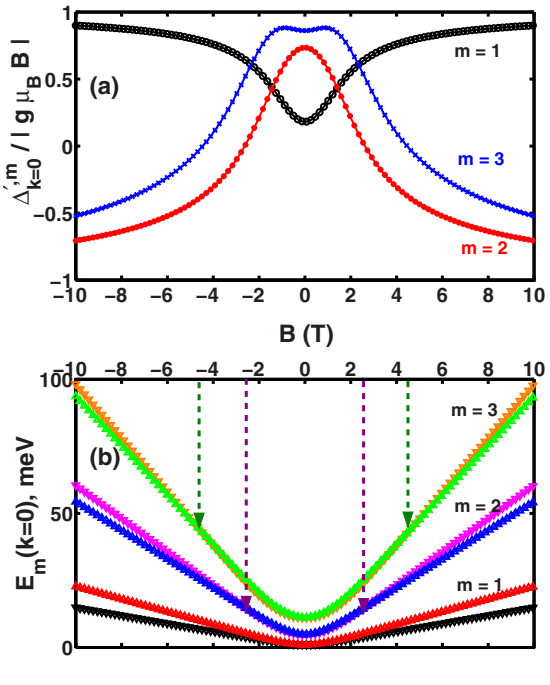

FIG. 7. (Color online) Zero-k spin splitting vs the external magnetic flux density B. We assumed that $\eta_R = 6\gamma_D = 3 \times 10^{-11}$ eV m. Other parameters are the same as before. (a) This figure shows the zero-k spin splitting energy $[\Delta'_m(k=0)]$ of subband m as a function of B. (b) Variation of the energy at subband bottom [i.e., $E_m(k=0)$] with B. Spin-split levels of subband 1 do not cross each other at any B. However, for subbands 2 and 3, such crossings occur at $B = 2.65$ T and $B = 4.45$ T, respectively, as shown by the dotted vertical arrows. At precisely these values of the magnetic flux density, the zero crossings occur in the top panel.

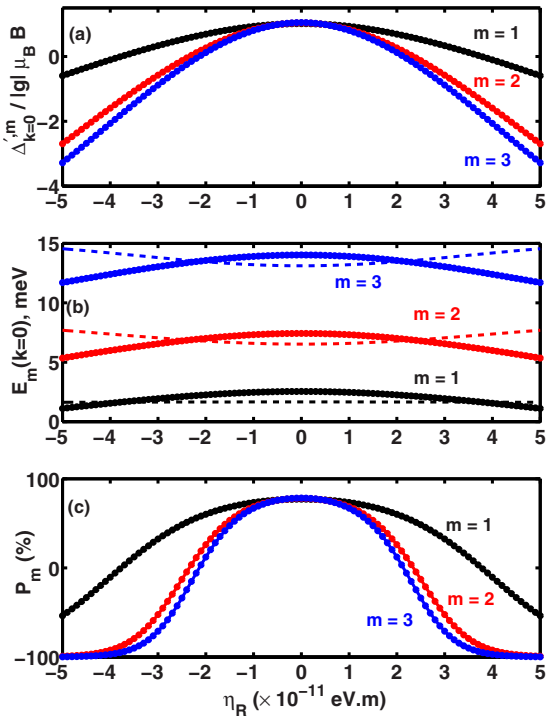

FIG. 8. (Color online) (a) The zero-k spin splitting energy $(\Delta'^{,m}_{k=0})$ in the lowest three subbands as a function of the Rashba interaction strength η_R. This quantity decreases and eventually flips sign as the magnitude of the Rashba interaction strength $(|\eta_R|)$ is increased. The Dresselhaus constant γ_D has a fixed value of 0.5×10^{-11} eV m, and the external magnetic flux density $B = 1$ T. This figure also shows that $\Delta'^{,m}_{k=0}$ is an even function of η_R. (b) Variation of the energy at the bottom of each spin-split level in the lowest three subbands with η_R. The two spin levels are denoted by solid and broken lines. In each subband, the spin levels cross at some value of $|\eta_R|$, which gives rise to the zero crossings in the top panel. (c) The equilibrium spin polarizations of carriers in the lowest three subbands as functions of η_R at temperature $T = 5$ K.

the magnitude and sign of the g factor, and the effective mass), the energy at the bottom of the lower spin level in subband 1 increases *slower* with the magnetic field (increasing magnetostatic confinement) than the energy at the bottom of the upper spin level. As a result, the spin splitting energy continues to increase with increasing magnetic field. However, in subbands 2 and 3, the energy of the lower spin level increases *faster* with increasing magnetic field than the energy of the upper spin level. Therefore, the lower spin level soon overtakes the upper spin level (causing the zero crossing), and thereafter a role reversal takes place whereby the lower level actually has higher energy than the upper level. This makes the spin splitting energy negative. The designation "lower" or "upper" spin level is determined by which level is lower at $B \to 0$.

IV. GATE CONTROL OF SPIN POLARIZATION

In Fig. 8(a), we show the zero-k spin splitting $\Delta'^{,m}_{k=0}$ in the three lowest subbands as a function of the Rashba interaction strength η_R for a fixed value of γ_D $(0.5 \times 10^{-11}$ eV m) and $B = 1$ T. Note that $\Delta'^{,m}_{k=0}$ is an even function of η_R, meaning that it does not depend on the direction of the symmetry-breaking electric field inducing the Rashba interaction. Note also that there are zero crossings here as well. To explain that, we have plotted in Fig. 8(b) how the subband bottom energies evolve with increasing η_R. The solid and broken lines denote the two spin-split levels. At $\eta_R = 0$, the spin splitting energy is nearly $g\mu_B B$ since γ_D is very small and can be ignored. Because the g factor is negative, the spins in the lower level are aligned antiparallel to the external magnetic field (everywhere, independent of the z coordinate), and those in the upper level are aligned parallel to the external magnetic field (also independent of the z coordinate) when $\eta_R = 0$. As $|\eta_R|$ increases, the spin orientations change and become z dependent. Interestingly, the original lower level increases in energy while the upper level decreases. This is shown clearly in Fig. 8(b), which also shows the zero crossings.

The zero-k spin splitting energy has a strong dependence on η_R, which can be varied by applying an electrostatic field in the y direction with a top gate terminal. Now, let us assume that the Fermi level in the quantum wire is well below the lowest subband $(m = 1)$ so that the carrier population is nondegenerate. The electrons will occupy the states in the vicinity of subband bottom since the density of states in a

quasi-one-dimensional system has a van Hove singularity at the subband bottom. Accordingly, the (spatially averaged) spin polarization of the carriers in the mth subband can be approximated as

$$P_m = \frac{n_\uparrow - n_\downarrow}{n_\uparrow + n_\downarrow} = \tanh\left[\frac{\Delta'^{,m}_{k=0}}{2k_BT}\right], \tag{26}$$

where $\uparrow$ and $\downarrow$ refer to the (spatially averaged) eigenspinors in the two spin-split bands in the mth subband at $k=0$ and k_B is the Boltzmann constant. Since $\Delta'^{,m}_{k=0}$ depends on the strengths of the Rashba and Dresselhaus spin-orbit interaction strengths, we can vary $\Delta'^{,m}_{k=0}$—and therefore the spin polarization in any subband of the quantum wire—with external gate potentials. In Fig. 8(c), we show the spin polarization P_m in the lowest three subbands of the quantum wire as a function of η_R. Clearly, we can vary P_m (and even invert its sign) if we change η_R with a gate potential. The spin polarization can also be varied with the external magnetic field, but since an electric field can be switched much faster than a magnetic field, the electrostatic control is always preferable.

V. CONCLUSION

In conclusion, we have calculated the energy dispersion relations of the spin-split subbands in a quantum wire subjected to a transverse magnetic field in the presence of spin-orbit coupling. We have shown that the zero-k spin splitting in any subband is not the bare Zeeman splitting and not linear in the magnetic field. The zero-k spin splitting is also subband dependent. Similar subband dependence has also been reported in Ref. 7. Particularly, the magnetic field dependence of the zero-k spin splitting is intriguing since it could become zero in some subbands at a nonzero value of the magnetic field. It can also exhibit sign changes as the magnetic field is varied. Finally, we have shown that the zero-k spin splitting in any subband can be modulated with an external gate potential, which allows us to control the net spin polarization in the wire by electrical means. The modulation of the spin-splitting energy with a gate voltage has applications in quantum computing.[22]

*Author to whom correspondence should be addressed; sbandy@vcu.edu

[1] A. V. Moroz and C. H. W. Barnes, Phys. Rev. B **60**, 14272 (1999).
[2] W. Häusler, Phys. Rev. B **63**, 121310(R) (2001).
[3] E. A. de Andrada e Silva and G. C. La Rocca, Phys. Rev. B **67**, 165318 (2003).
[4] M. Cahay and S. Bandyopadhyay, Phys. Rev. B **68**, 115316 (2003).
[5] M. Cahay and S. Bandyopadhyay, Phys. Rev. B **69**, 045303 (2004).
[6] S. Bandyopadhyay, S. Pramanik, and M. Cahay, Superlattices Microstruct. **35**, 67 (2004).
[7] S. Debald and B. Kramer, Phys. Rev. B **71**, 115322 (2005).
[8] M. Zarea and S. E. Ulloa, Phys. Rev. B **72**, 085342 (2005).
[9] J. Knobbe and Th. Schäpers, Phys. Rev. B **71**, 035311 (2005).
[10] S. Zhang, R. Liang, E. Zhang, L. Zhang, and Y. Liu, Phys. Rev. B **73**, 155316 (2006).
[11] X. W. Zhang and J. B. Xia, Phys. Rev. B **74**, 075304 (2006).
[12] C. A. Perroni, D. Bercioux, V. Marigliano Ramaglia, and V. Kataudelca, J. Phys.: Condens. Matter **19**, 186227 (2007).
[13] J. Sun, S. Gangadharaiah, and O. A. Starykh, Phys. Rev. Lett. **98**, 126408 (2007).
[14] J. Nitta, T. Akazaki, H. Takayanagi, and T. Enoki, Phys. Rev. Lett. **78**, 1335 (1997).
[15] S. Bandyopadhyay and M. Cahay, Appl. Phys. Lett. **85**, 1814 (2004).
[16] E. I. Rashba, Sov. Phys. Solid State **2**, 1109 (1960); Y. A. Bychkov and E. I. Rashba, J. Phys. C **17**, 6039 (1984).
[17] G. Dresselhaus, Phys. Rev. **100**, 580 (1955).
[18] E. N. Bulgakov and A. F. Sadreev, Phys. Rev. B **66**, 075331 (2002).
[19] S. Chaudhuri and S. Bandyopadhyay, J. Appl. Phys. **71**, 3027 (1992).
[20] J. Wan, M. Cahay, and S. Bandyopadhyay, J. Nanoelectron. Optoelectron. **1**, 60 (2006).
[21] See, for example, M. Governale and U. Zülicke, Phys. Rev. B **66**, 073311 (2002).
[22] S. Bandyopadhyay, Phys. Rev. B **61**, 13813 (2000).